Numerical Solutions of Vascular Repair : assessing bypasses of an iliac artery obliteration

A. R. Ghigo[a], S. Abou Taam[a,b], X. Wang[a], P-Y Lagrée[a], J-M Fullana[a]
[a] Sorbonne Universités, UPMC Univ Paris 06
CNRS, UMR 7190, Institut Jean Le Rond d'Alembert, F-75005 Paris
[b] Hôpital Privé Claude Galien, 91480 Quincy-Sous-Sénart

Résumé : *Nous présentons un modèle numérique pour l'écoulement 1D de sang dans un réseau artériel dans l'objectif d'étudier les performances de trois différents pontage d'une pathologie aiguë, la sténose de l'artère iliaque. Les simulations numériques montrent que les trois pontages aident à récupérer le flux artériel normal en aval du pontage.*

Abstract : *We propose an arterial model based on 1D hemodynamic equations to study the performances of different vascular surgical repairs in case of occlusive pathologies. The occlusive pathology is an iliac artery obliteration or stenosis and we define three different bypasses to restore the blood flow after the stenosis. Numerical simulations show that all bypass grafts have similar success since we retrieve the normal hemodynamics after the bypass graft.*

Key words : arterial network, 1D model

1 Introduction

We propose a help-to-decision tool for evaluating the performances of vascular surgical repairs in case of occlusive pathologies. The study case we present is an iliac artery obliteration which can be defined as an important stenosis or narrowing of the cross sectional area of an artery, resulting in a small or negligible flow rate after the obliteration. The obliteration of an iliac artery is a severe pathology since it carries most of blood flow to the lower member. The ischemia is due to the decrease of blood flow in tissues when the vessel providing vascularization is narrowed or occluded, and such arterial lesions can have severe consequences such as amputation if the blood flow is not restored in time.

The available surgical solutions are simple and consist in performing bypass graft surgeries or anastomoses to redirect the blood flow from another healthy artery to bypass the obliterated vessel and restore the blood flow after the stenosis. However, in presence of a middle stenosis, endoprosthesis, i.e. a hollow stent inserted into the artery is the most used treatment. For an iliac artery obliteration there are three typical configurations of bypass graft: aortofemoral, axillofemoral and cross-over femoral, defined by

the name of the healthy artery where the proximal anastomosis is performed (aorto for aorta, axillo for axillary and cross for the same artery on the opposite leg).

The aim of this communication is to present a numerical model of an arterial network presenting this pathology and to compute numerical solutions of the blood flow after the bypass graft surgery is performed. We hope that this work can help the medical staff optimize surgical repair (i) by predicting the flow rate and pressure evolution after the bypass graft and (ii) by assessing the global flow rate in the opposite member which is an aposteriori evaluation of the quality of the bypass.

(a)

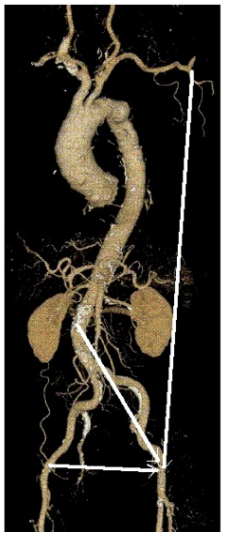

(b)

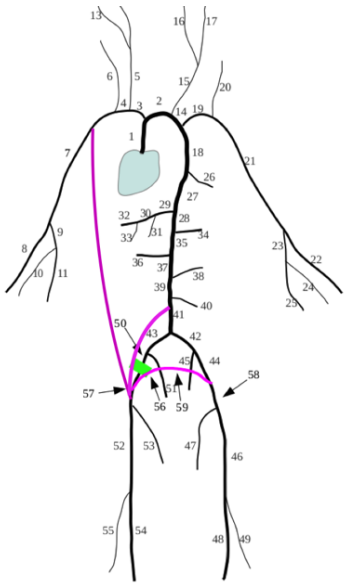

Figure 1: Arterial trees. (a) Angioscan of part of the arterial network with the three bypasses in solid lines. (b) Equivalent numerical model : the narrowing the iliac artery is marked in green and the bypass grafts in purple.

We build the numerical model of the arterial network by connecting arterial segments following the model of a real angioscan of the principal arteries of the great circulation (55 segments). This arterial tree is know in the literature as the basic model of the systemic network. The Figure 1 (a) presents a MRI where the three bypasses are marked using solid lines. The equivalent numerical network is shown in Figure 1 (b) where the pathology is modeled by narrowing the principal artery of the lower leg, the iliac artery (green mark in Figure 1 (b)). The artery numbers where the proximal and distal anastomoses are performed are : aortofemoral (41 and 57), axillofemoral (7 and 57) and cross-over femoral (44 and 57, purple line on Figure 1 (b)).

The hemodynamic flow through each segment follows a 1D numerical model which can be expressed in terms of averaged values, the cross-sectional area A and the flow rate Q. We present the numerical model in Section 2 and the results in the following sections.

2 Numerical Model

We use the 1D governing equations for blood flow expressed using the dynamical variables of flow rate Q, cross-sectional area A and internal average pressure P. The 1D equations come from the integration over the cross-sectional area of the Navier-Stokes equations of an incompressible fluid at constant viscosity, giving the following mass and momentum 1D conservation equations

$$\frac{\partial A}{\partial t} + \frac{\partial Q}{\partial x} = 0, \tag{1}$$

$$\frac{\partial Q}{\partial t} + \frac{\partial}{\partial x}\left(\frac{Q^2}{A} + \frac{\beta}{3\rho}A^{\frac{3}{2}}\right) = -C_f\frac{Q}{A} + C_v\frac{\partial^2 Q}{\partial^2 x}, \tag{2}$$

where ρ is the density of the fluid and A_0 is the neutral cross-section area for a transmural pressure P_t equal to zero. The transmural pressure is defined as the difference between the internal or fluid pressure P and the external pressure P_{ext}

$$P = P_{ext} + \beta(\sqrt{A} - \sqrt{A_0}) + \nu_s\frac{\partial A}{\partial t}, \tag{3}$$

where β is related to the wall elasticity and ν_s to the visco-elasticity of the wall. We assumed here that the arterial wall is thin, isotropic, homogeneous, incompressible, and moreover that it deforms axisymmetrically with each circular cross-section independently of the others. We also used a Kelvin-Voigt model to describe the visco-elastic behavior of the wall [2]. It is straightforward to see that the coefficients

$$\beta = \frac{\sqrt{\pi}Eh}{(1-\eta^2)A_0} \quad \text{and} \quad C_v = \frac{\sqrt{\pi}\phi h}{2\rho(1-\eta^2)\sqrt{A_0}}$$

in equation (2) respectively incorporate the elastic behavior and the visco-elastic behavior of the wall dynamics of the problem. In this approach we defined $C_v = \frac{A\nu_s}{\rho}$ and used the Young's modulus E, the Poisson ratio η, the viscoelastic coefficient ϕ and the arterial thickness h. More details can be found in reference [1].

From a mathematical point of view the system of equation here presented is composed by an hyperbolic (transport equation, the l.r.s.) and an parabolic part (source term). Each part needs a specific integration scheme. The hyperbolic part was solved by a finite volume scheme (monotonic upwind scheme for conservation law, MUSCL) and the parabolic part by a Crank-Nicolson scheme. The implementation of the schemes has been verified using analytic solutions of a linearized system and experimental data [1, 3].

The connection between each segment of the network takes place at the branching points, where we considered a simple problem: a parent vessel with two daughter arteries. At the branching point, there are then six unknowns at the iteration $n+1$, A_p^{n+1} and Q_p^{n+1} for the outlet of the parent artery and $A_{d_1}^{n+1}$, $Q_{d_1}^{n+1}$,$A_{d_2}^{n+1}$ and $Q_{d_2}^{n+1}$ for the inlets of the two daughter arteries. All these quantities are function the the values at the iteration n. The pressures P_p^{n+1} and $P_{d_i}^{n+1}$ are expressed as a function of the cross-sectional area A using the constitutive relation relating the pressures and the cross-sectional area (equation (3)). From the physical point of view, we preserve the conservation of mass flux

$$Q_p^{n+1} - Q_{d_1}^{n+1} - Q_{d_2}^{n+1} = 0,$$

and the conservation of momentum flux

$$\frac{1}{2}\rho\left(\frac{Q_p^{n+1}}{A_p^{n+1}}\right)^2 + P_p^{n+1} - \frac{1}{2}\rho\left(\frac{Q_{d_i}^{n+1}}{A_{d_i}^{n+1}}\right)^2 - P_{d_i}^{n+1} = 0$$

There should be some terms for energy losses due to the branching but, in practice, these losses only have secondary effects on the pulse waves [2]. The last three equations needed to complete the resolution of the branching point problem come from the matching of the incoming and outgoing characteristics at the conjunction point. Finally the boundary conditions are: (i) an imposed physiological flow rate at the principal artery starting from the heart and (ii) reflection coefficients which is a model characterizing the resistance of the vascular bed.

3 Results

The key point of clinical repair is to restore the blood flow into the non perfused region, and secondarily, to avoid that this ill-balances the rest of the hemodynamic circulation. The network model presented above is able to capture both local and global phenomena. Our protocol is to simulate first a "healthy" network used as target, and second, a pathological one by narrowing the principal artery of the lower leg, the iliac artery (green mark in Figure 2 (b)). Later we apply the bypass grafts to the pathological network and compare blood flux and pressures over all the network against the target data (the "healthy" network). It is important to notice that numerical simulations allow access to all dynamic variables (pressure, cross sectional area, flow rate) simultaneously over the entire network, and that these data are not frequently available in clinical routine. We recall the main objective of this numerical study, (i) to assess the new hemodynamic conditions for each bypass to understand the modified flow hemodynamics and then (ii) to help medical staff to decide which one is better.

For each numerical simulations, healthy (normal network), pathological (iliac obliteration) and bypasses (aortofemoral, axillofemoral and cross-over femoral) we compute flow rate and pressure evolution in the segment distal to the iliac artery. The mechanical characteristic of the bypass graft, such as the compliance, the length and diameter, are taken from the literature [4]. In general the bypass is made in polytetylene terephthalate (Dacron), and has a diameter of 0.8 cm.

We present first the case of axillofemoral bypass graft, where the donor is the axillary artery of the same side than the occlusion. The Figure 2 shows a typical signal of flow rate (left) and pressure (right) at the iliac artery just after the occlusive site, for three situations : healthy (thin blue line), pathological (rel line) and repaired (dotted blue line). We observe that both the flow rate and the pressure decrease when the artery is occluded, and that normal values are retrieved when the bypass graft is connected. The position of the each peak (or phase shift) is due to the different distances traveled by the waves.

To assess the results of the simulation we define an index as the ratio of the integrated flow rate over one time-period for each artery to the integrated flow rate over one period at the inlet. This index is evaluated at different positions along the network: (i) twice at

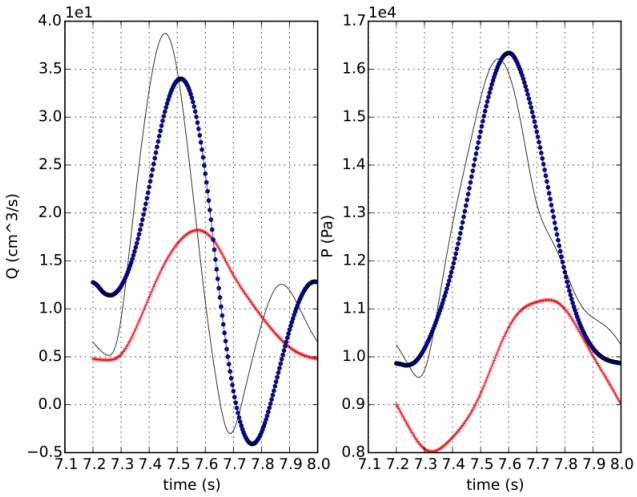

Figure 2: Flow rate (left) and pressure (right) for healthy (thin black line), pathological (rel line) and repaired (dotted blue line) situations at the iliac artery.

the iliac artery, before and after the obstruction zone, (ii) in the opposite lower leg and (iii) in the arm after the bypass graft. The Table 1 shows a summary of the numerical results: the first row shows that in a normal or healthy case 10.2% of the input integrated flow rate goes to the lower right leg (the same amount goes to the lower left leg – see 2nd row–) and falls down to 7.9% when the iliac is obstructed. After bypass surgery the lower right leg recovers the normal circulation, and we can note that the flow rate in the Right Subclavian I artery doubles since it now also irrigates the right leg. On the contrary, the rest of the hemodynamic system (i.e. arm and opposite leg) is not affected very much by the prensce of the bypass graft.

Position	Number	Normal	Obst.	Bypass
Right Iliac (before)	43	10.2%	7.9%	0.9%
Left Iliac	42	10.3%	10.6%	10.3%
Right Iliac (after)	52	9.4%	7.1%	9.3%
Right Subclavian I	7	10.5%	10.7%	19.6%
Right Ulnar II	8	4.3%	4.5%	4.3%

Table 1: Results in terms of % of total flow rate for axillofemoral bypass. Column Number corresponds to the artery numbers of Figure 1 (b)

The second bypass studied, the cross-over femoral bypass, connects, as mentioned before, the obstructed iliac artery with the similar artery in the opposite leg. The Table 2 shows the results of the simulation. Since now the donor artery carries the supplement of flow rate necessary, the flow rate increases as proved by the doubling of the Left Iliac values (10.3% to 19.65%) just before the anastomosis. A normal hemodynamic circulation is retrieved after bypass.

Position	Number	Normal	Obst.	Bypass
Right Iliac (before)	43	10.2%	7.9%	0.85%
Left Iliac	42	10.3%	10.6%	19.65%

Table 2: Results in terms of % of total flow rate for cross-over femoral bypass. Column Number corresponds to the artery numbers of Figure 1 (b)

The general behavior of the last bypass, the aortofemoral (not shown here), is in fact the same as the others.

4 Conclusion

We presented numerical simulations of an iliac artery obliteration. The aim of our approach is to provide an help-to-decision tool to assess vascular surgical repair of occlusive pathologies. We computed the blood flow in a network where the three classical bypasses for an iliac obliteration were performed, using the network parameters of an "average" man and the mechanical characteristics of the bypass taken from the literature. Numerical simulations show that all bypass grafts have similar success since we retrieve the normal hemodynamics after bypass graft. This result suggests that both the mechanical characteristic and the diameter of the bypass are well dimensioned as long as the hemodynamic conditions are recovered. Concerning this point it will be useful to do parametric analysis for understanding the limits, both mechanical and geometrical, of the bypass in order of optimize them.

Numerical prediction could be used to optimize or plan surgeries for specific patients, if the pathologies are well defined and the physiologic parameters known.

References

[1] X. Wang et al. *Verification and comparison of four numerical schemes for a 1D viscoelastic blood flow model*, Computer Methods in Biomechanics and Biomedical Engineering, 2015.

[2] Alastruey, J. et al. *Pulse wave propagation in a model human arterial network: Assessment of 1-D visco-elastic simulations against measurements*, Journal of Biomechanics, 2011.

[3] M. Saito et al. *One-Dimensional Model for Propagation of a Pressure Wave in a Model of the Human Arterial Network: Comparison of Theoretical and Experimental Results*, Journal of Biomechanical Engineering, 2011.

[4] S. Sarkar et al. *The Mechanical Properties of Infrainguinal Vascular Bypass Grafts: Their Role in Influencing Patency*, Eur. J. Vasc. and Endovascular Surgery, 31, 6, 2006.